THEORETICAL BACKGROUND AND VERIFICATION OF THE P-Y METHOD IMPLEMENTATION IN DEEPFND/HELIXPILE SOFTWARE

DeepFND software program

Document Version 1.2.0.1

Issued: 10-Jan-2016
Revised: 13-Jul-2021

Deep Excavation LLC

www.deepexcavation.com

www.deepex.com

Table of Contents

Introduction

The following report contains the theoretical background of the P-Y modeling approach implemented in the HelixPile and DeepFND software. The current report consists of a detailed literature review on the different P-Y models along with the verification of the P-Y modeling method implementation in HelixPile with a number of published experimental results.

1. Simulation of pile foundations

The lateral analysis in the HelixPile and DeepFND software is accomplished through the construction of P-Y models as illustrated in figure 1.1. As presented in the figure the pile is simulated as a Euler-Bernoulli beam with either elastic or inelastic properties, defined by the user. The pile beam is discretized in accordance to a predefined mesh and a P-Y spring is assigned to each pile node beneath the soil surface. The P-Y spring is defined by a pressure to displacement relationship or force to displacement relationship through multiplication of the pressure term with the tributary area of the node.

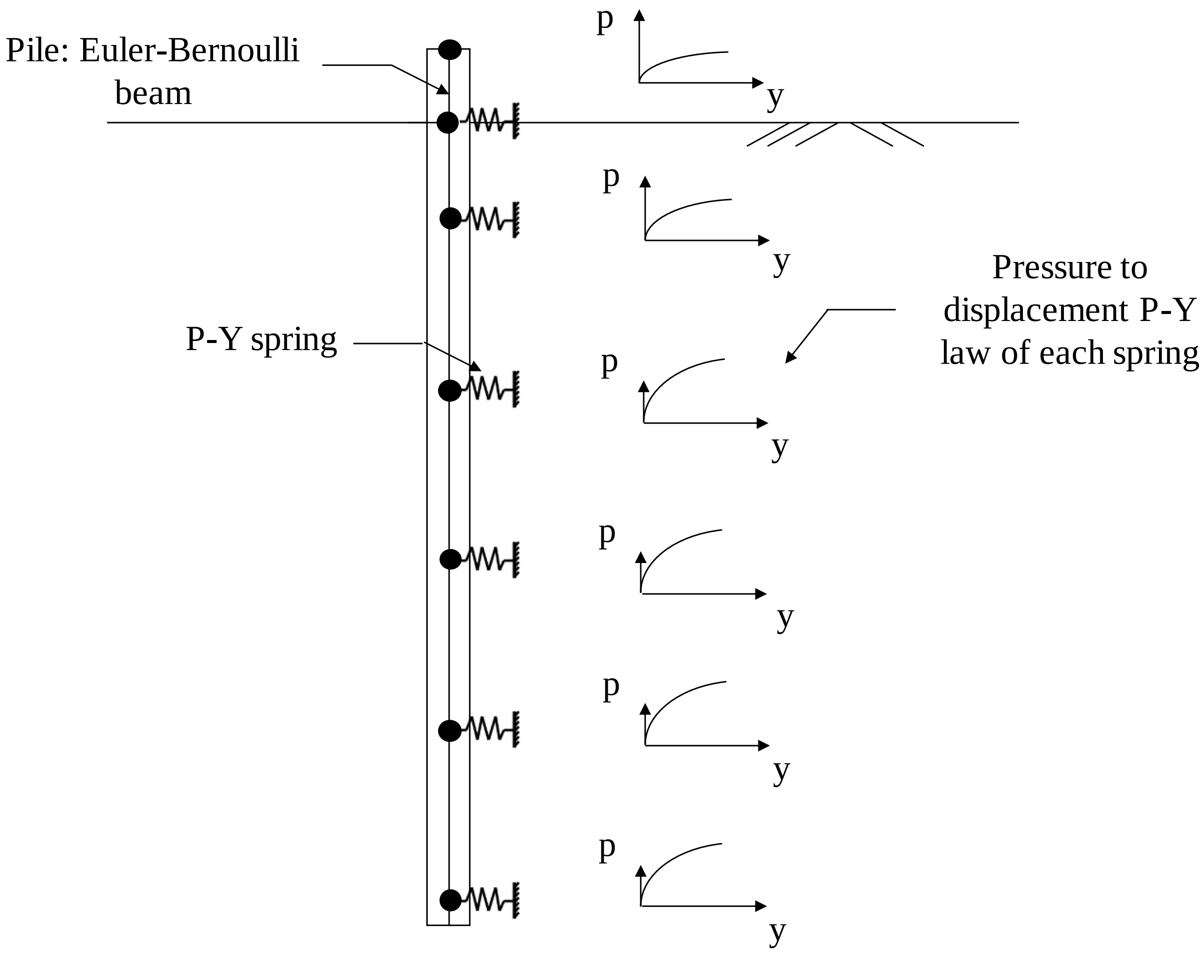

Figure 1.1: Illustration of lateral P-Y model

2. Implementation of P-Y method

All the methods discussed in the following paragraph are either generated from full scale or centrifuge experiments or follow a mathematical derivation efficiently calibrated through the use of full scale or centrifuge experiments. The following section presents the different P-Y models implemented in DeepFND and HelixPile software for different soil properties along with the appropriate adjustments on the models for the consideration of the multilayer soil profile and the battering pile scenarios.

2.1 Soil Models

2.1.1 soft clay model (Matlock)

On the consideration of a pile foundation located in a soft clay soil a P-Y relation was published by Matlock in 1970. The backbone curve is described by three individual parts among which the first is linear the second parabolic while the 3rd is constant. The backbone curve along with its mathematical formulation is illustrated below.

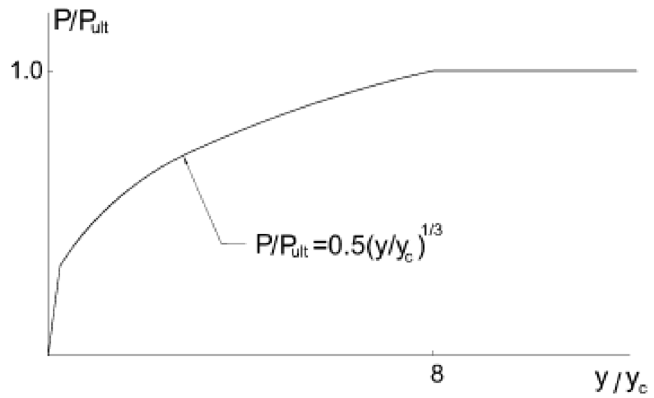

Figure 2.1: Matlock P-Y relation for soft clays under static loading

The proposed backbone curve was generated from experiments in soft clay sand and as a result the method can be applied on soil layers with such properties. The parameters P_{ult} and y_c can be directly calculated from the following formulas.

$$p_u = 3c + \gamma X + J\frac{cX}{D} \tag{1}$$

$$p_u = 9c \quad for \;\; X \geq X_R \tag{2}$$

On the notation of the aforementioned equations p_u is the ultimate resistance of the soil, c is the undrained shear strength for undisturbed clay, *D* is the pile diameter, *γ* is the effective unit weight of the soil, *J* is a dimensionless empirical constant with values ranging from 0.25 to 0.5, *X* is the depth below the soil surface while X_R is the depth below soil surface to bottom of the reduced resistance zone calculated from the following equation.

$$X_R = \frac{6D}{\frac{\gamma D}{c} + J} \tag{3}$$

The calculation of y_{50} is accomplished through the following equation where ε_c is the strain which occurs at one half the maximum stress on laboratory undrained compression tests of undisturbed soil samples (equal to 0.005 as proposed by Matlock for soft clays).

$$y_c = 2.5\varepsilon_c D \tag{4}$$

As observed on cyclic loading experiments (Matlock 1978) the PY relation is considered to have some differences with the bearing capacity been reduced to 72% and the last term of the PY relation close to the surface having a descending behavior instead of a constant one. The cyclic Matlock model equations and graph are illustrated in the following figure.

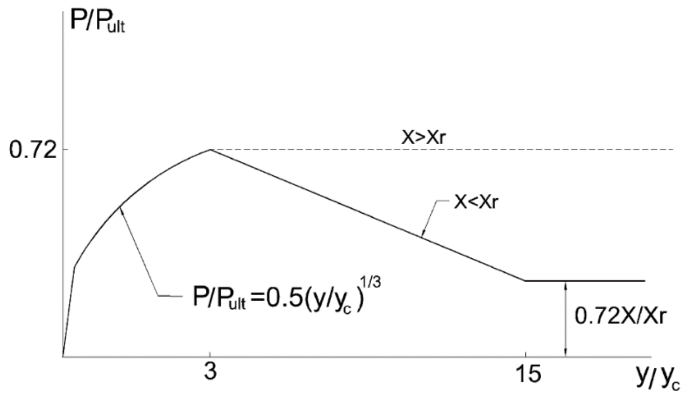

Figure 2.2: Matlock P-Y relation for soft clays under cyclic loading

2.1.2 sand model (API 1993)

The API 1993 method can describe a single pile foundation located in a sand soil environment. The relationship follows a hyperbolic exponential P-Y relation according to the following equation.

$$P = A \cdot p_u \cdot \tanh\left[\frac{k \cdot H}{A \cdot p_u} y\right] \tag{5}$$

Pu is the ultimate strength of the soil; *k* is the initial modulus of subgrade reaction and *H* is the depth. Coefficient *A* takes into account the change of behavior from static to quasi static loading and can be calculated from the following equation.

$$\begin{aligned} &A = 0.9 && \textit{for cyclicloading} \\ &A = \left(3 - 0.8\frac{H}{D}\right) \geq 0.9 && \textit{for static loading} \end{aligned} \tag{6}$$

The values P_u and y_{50} can be either calculated from the appropriate measurements on site or through the use of the proposed simplified calculations of API 2000. The calculation can be accomplished through the following equations.

$$P_{us} = (C_1 \cdot H + C_2 \cdot D) \cdot \gamma \cdot \mathrm{H} \tag{7}$$

$$P_{u\delta} = C_3 \cdot D \cdot \gamma \cdot \mathrm{H} \tag{8}$$

Where *Pu* is the ultimate resistance (s=shallow, d=deep), *γ* is the effective soil weight, *H* is the depth of the location in calculation, *φ'* is the angle of internal friction of the sand and *D* the average pile diameter from surface to depth. Coefficients C1, C2 and C3 and the initial modulus of subgrade reaction can be calculated by the following graphs.

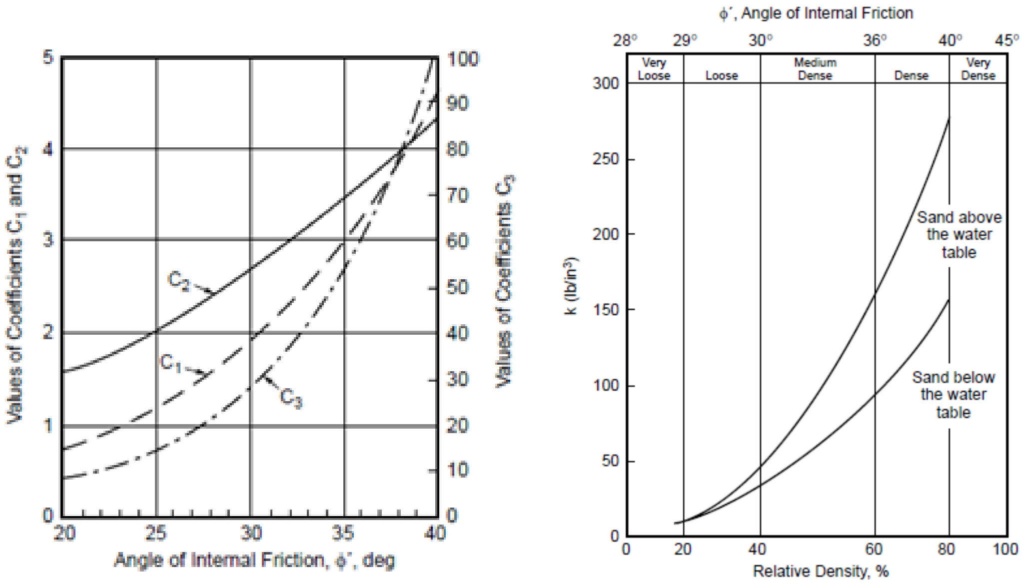

Figure 2.3: calculation of a)coefficients C1,C2,C3 from angle φ' b) modulus of subgrade reaction from internal friction angle φ'as depicted in API 2000.

2.1.3 Stiff Clay Model in the presence of free water

For the scenario of a stiff clay soil profile in the presence of free water, a representative P-Y model was developed by Reese et al (Reese et al 1975) in accordance to the results of the Manor site experiments. The displacement reaction law of the specific model is described by four individual portions. Prior to the calculation of each portion of the reaction displacement law it is essential to calculate the ultimate soil resistance of the soil for the specific depth for the two different mechanisms of wedge and flow failure.

$$P_{ct} = 2c_a D + \gamma' D z + 2.83 c_a z \tag{9}$$

$$P_{cd} = 11 c_u D \tag{10}$$

Where D is the diameter of the pile, γ' the effective density factor, z the depth under study, c_a the average undrained shear strength over depth z and c_u the undrained shear strength. The calculation of each portion for the scenario of static loading combination is accomplished through equations 11, 12, 13, 14 and 15 for each individual portion respectively.

$$p = (k \cdot z) \cdot y \tag{11}$$

$$p = 0.5 \cdot p_u \cdot \left(\frac{y}{y_{50}} \right)^{0.5} \tag{12}$$

$$p = 0.5 \cdot p_u \cdot \left(\frac{y}{y_{50}} \right)^{0.5} - 0.055 \cdot p_u \left(\frac{y - A_s \cdot y_{50}}{A_s \cdot y_{50}} \right)^{1.25} \tag{13}$$

$$p = 0.5 \cdot p_u \cdot \left(\frac{y}{y_{50}} \right)^{0.5} - 0.411 \cdot p_u - \frac{0.0625}{y_{50}} \cdot p_u \left(y - 6A_s \cdot y_{50} \right) \tag{14}$$

$$p = 0.5 \cdot p_u \cdot \left(\frac{y}{y_{50}} \right)^{0.5} - 0.411 \cdot p_u - 0.75 \cdot p_u A_s \tag{15}$$

Where *k* is the initial subgrade reaction constant and A_s is the static resistance coefficient calculated from figure 5. The calculation of each portion for the scenario of cyclic loading combination is accomplished through equations 11, 12, 13, 16 and 17 for each individual portion respectively.

$$p = A_c \cdot p_u \cdot \left(1 - \left| \frac{y - 0.45 y_p}{0.45 y_p} \right|^{2.5} \right) \quad where \quad y_p = 4.1 \cdot A_c \cdot y_{50} \tag{14}$$

$$p = 0.936 \cdot A_c \cdot p_u \cdot - \frac{0.085}{y_{50}} p_u (y - 0.6 y_p) \tag{16}$$

$$p = 0.936 \cdot A_c \cdot p_u \cdot - \frac{0.102}{y_{50}} p_u y_p \tag{17}$$

Where A_c is the cyclic resistance coefficient calculated from figure 5. The aforementioned P-Y model curves are illustrated in figure 4 for the scenario of a static and cyclic loading combination respectively.

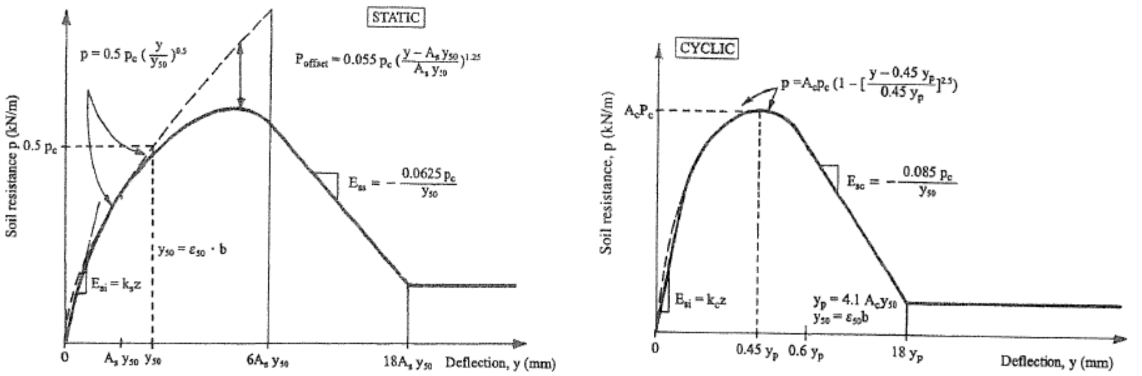

Figure 2.4: Stiff clay P-Y model in the presence of free water for a) static and cyclic loading conditions as proposed by Reese et al (1975)

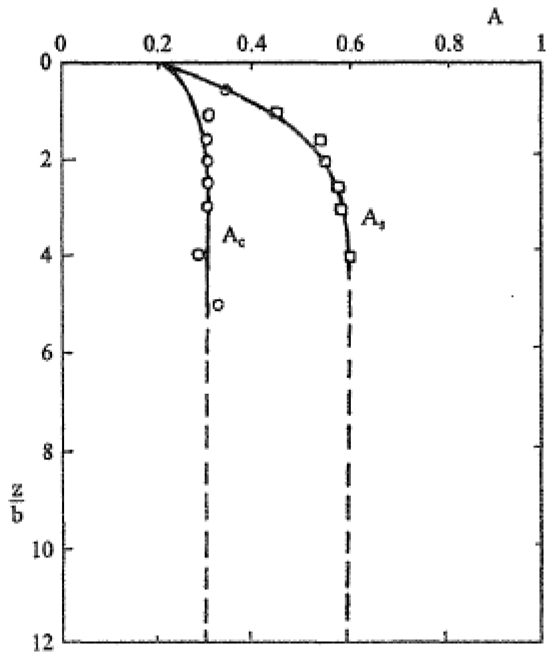

Figure 2.5: Soil resistance coefficients for the stiff clay P-Y model with free water a) for static and b) for cyclic loading conditions as proposed by Reese et al (1975)

2.1.4 Stiff Clay Model with no free water

On the scenario of a stiff clay layer with no free water Welch and Reese (Welch and Reese 1972) developed a P-Y model with properties according to the proposed backbone curve generated from experiments of bored pile in stiff clay located at a test site in Houston, Texas. The calculation of P_{ult} can be directly calculated from the minimum value of the following formulas.

$$p_u = \left[3 + \frac{\gamma' \cdot z}{c_u} + J\,\frac{z}{D}\right] \cdot c_u D \tag{18}$$

$$p_u = 9 c_u D \tag{19}$$

The overall reaction – displacement curve is defined by two different portions an initial parabolic and a following constant portion when the ultimate soil resistance has been reached. The calculation is accomplished through the following equations.

$$p = p_u \cdot 0.5\left(\frac{y}{y_{50}}\right)^{1/4} \quad for \;\; y > 16 y_{50} \tag{20}$$

$$p = p_u \qquad for \;\; y > 16 y_{50} \tag{21}$$

For the scenario of a cyclic loading combination Welch and Reese have proposed the appropriate adjustments on the model according to which the soil resistance decreases as the number of the loading cycles increases. The cyclic loading coefficients needed for the adjustments are calculated through the following equations.

$$C = 9.6\left(\frac{p}{p_u}\right)^4 \tag{22}$$

$$y_c = y_s + y_{50} C \log N \tag{23}$$

The displacement reaction curves of the p-y model derived by Welch and Reese is illustrated in figure 6 for the scenario of cyclic and static loading conditions.

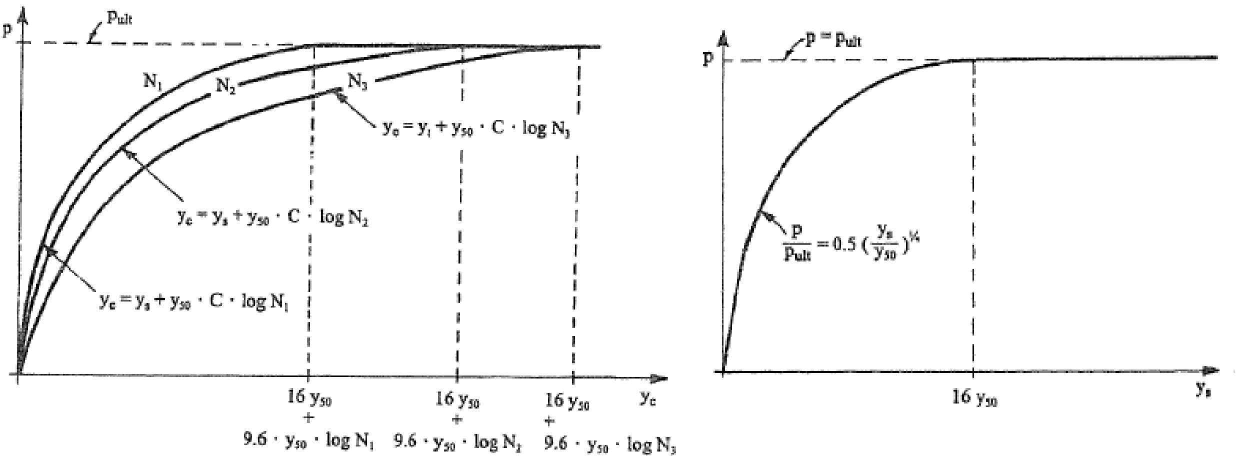

Figure 2.6: Stiff clay P-Y model with no free water for a) static and cyclic loading conditions as proposed by Welch and Reese(1972)

2.1.5 Sand soil model (Reese)

The soil model developed by Reese et al. (1974) is an alternative modeling approach for single piles located in soil sites consisting of sand. The Reese et al model is generated through the theoretical approach of wedge failure for the near surface depth and the flow failure for deeper cases. The soil resistance parameters are appropriately adjusted according to experiments performed in the test site on Mustang Island by Cox et al. (1974).

The soil resistance at a specific soil depth is calculated for the two scenarios of wedge failure and flow failure through the following equations and the minimum value is taken into account.

$$p_{st} = \gamma' \cdot z \left[\begin{array}{l} \dfrac{K_o z \tan\phi \cdot \sin\beta}{\tan(\beta-\phi)\cdot\cos a} + \dfrac{\tan\beta}{\tan(\beta-\phi)}\left(D + z\tan\beta\tan a\right) \\ + K_o z \tan\beta(\tan\phi\cdot\sin\beta - \tan a) - K_a D \end{array} \right] \tag{24}$$

$$p_{sd} = K_a D\gamma' \cdot z\left(\tan^8\beta - 1\right) + K_o D \cdot \gamma' \cdot z \tan\phi \tan^4\beta \tag{25}$$

$$\text{Where} \quad a = \phi/2 \quad \text{and} \quad \beta = 45 + \phi/2$$

The parameter K_a is the active pressure coefficient, K_o is the earth pressure coefficient at rest and ϕ is the soil friction angle. The actual soil resistance is calculated through the use of the adjustment factors A and B from the equations 26 and 27 along with the use of figure 8.

$$p_u = \overline{A} \min(p_{sd}, p_{st}) \tag{26}$$

$$p_m = B \min(p_{sd}, p_{st}) \tag{27}$$

The overall displacement reaction curve of the specific P-Y model is comprised by an initial linear portion according to the elastic behavior of the soil, a parabolic portion interpolating between the 1st and the 3rd portion, and finally a linear and constant portion at the level of the ultimate soil resistance. The formulas needed for the calculation of each portion are illustrated in the following equations.

$$p = k \cdot z \cdot y \tag{28}$$

$$p = \overline{C}\, y^{1/n} \tag{29}$$

$$m = \frac{p_u - p_m}{y_u - y_m} \tag{30}$$

$$n = \frac{p_m}{m \cdot y_m} \tag{31}$$

$$\overline{C} = \frac{p_m}{y_m^{1/n}} \tag{32}$$

$$y_k = \left(\frac{\overline{C}}{kz} \right)^{n/(n-1)} \tag{33}$$

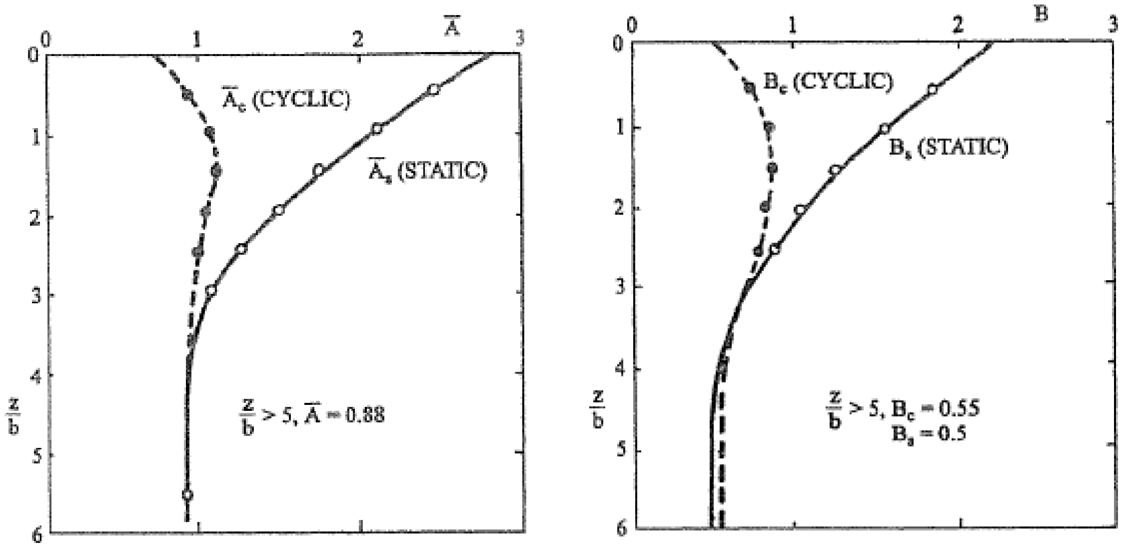

Figure 2.8: Soil resistance coefficients for the Reese sand P-Y model a) for static and b) for cyclic loading conditions as proposed by Reese (1974)

The displacement reaction curves of the p-y model derived by Reese for the scenario of sites consisting of sand soil is illustrated in figure 8.

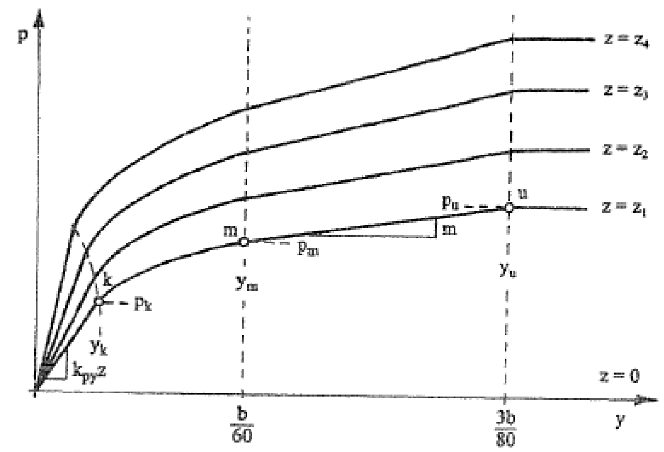

Figure 2.8 : Cohesionless soil P-Y model as proposed by Reese(1974)

2.1.6 Weak rock model

The soil model developed by Reese (1997) is capable of coping with single piles located in soil sites consisting of weak rock. The proposed backbone curve was generated from the results of two full scale experiments on site of bored piles in rock (Nyman 1980; D. Speer, unpublished report, 1992). According to the proposed method the ultimate soil resistance at each depth is calculated from the following equations taken into account the weaker properties of the rock layer surface.

$$p_{ur} = a_r q_{ur} b\left(1 + 1.4\frac{x_r}{b}\right) \qquad 0 \le x_r \le 3b \tag{34}$$

$$p_{ur} = 5.2 a_r q_{ur} b \qquad x_r \ge 3b \tag{35}$$

The parameter q_{ur} corresponds to the compressive strength of rock, usually lower-bound as function of depth, a_r corresponds to a strength reduction factor calculated from figure 9a, b is the pile diameter and x_r the depth in question below surface. The calculation of the initial modulus of the P-Y curve is accomplished through the following equations.

$$K_{ir} = k_{ir} E_{ir} \tag{36}$$

$$k_{ir} = \left(100 + \frac{400 x_r}{3b}\right) \qquad 0 \le x_r \le 3b \tag{37}$$

$$k_{ir} = 500 \qquad x_r \ge 3b \tag{38}$$

The parameter E_{ir} corresponds to the initial modulus of the rock soil while b is the diameter of the pile. The backbone curve consist of an initial portion according to the modulus Kir followed by a parabolic portion leading to the final constant branch at the ultimate soil resistance level.

$$p = K_{ir} y \qquad y \le y_A \tag{39}$$

$$p = \frac{p_{ur}}{2}\left(\frac{y}{y_{rm}}\right)^{0.25} \quad y \ge y_A \qquad p \le p_{ur} \tag{40}$$

$$p = p_{ur} \tag{41}$$

The essential parameter y_{rm} and y_a can be calculated from the equations 42 and 43.

$$y_{rm} = k_{rm} b \tag{42}$$

$$y_A = \left[\frac{p_{ur}}{2 y_{rm}^{0.25} K_{ir}} \right]^{1.333} \tag{43}$$

The displacement reaction curves of the p-y model derived by Reese for the scenario of sites consisting of weak rock along with the modulus reduction ratio function of RQD as proposed by Blenlawski are illustrated in figure 9.

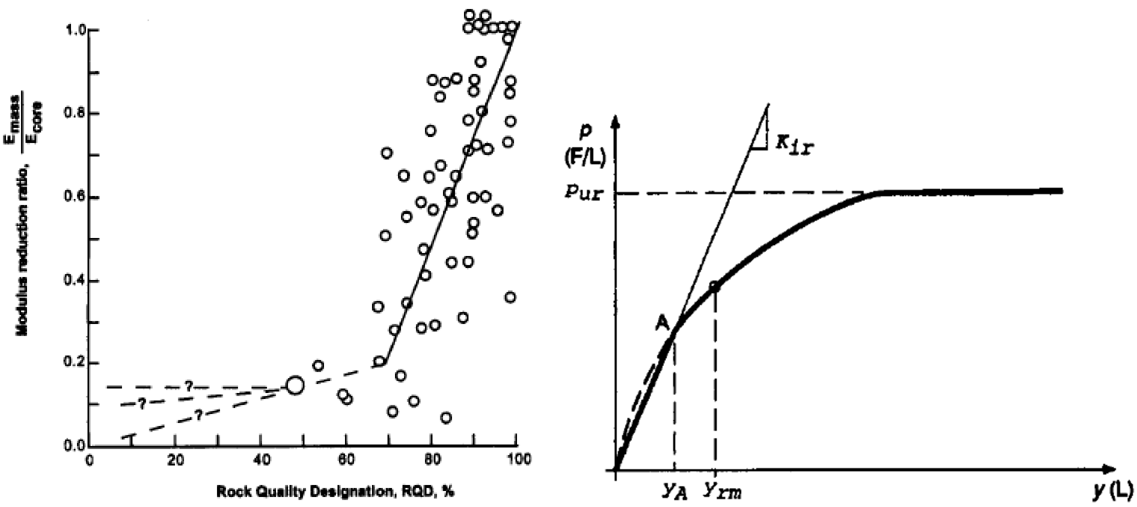

Figure 2.9: a) modulus Reduction Ratio Function of RQD after Blenlawski (1984) b) weak rock soil P-Y model as proposed by Reese(1997)

2.1.7 Silt soil Model

On the scenario of a site consisting of silt soil deposits, Reese and Van Impe (2001) proposed an appropriate simulation model for the P-Y method. The procedure to develop p-y curves for c-ϕ soil was suggested based upon procedure in developing p-y curves for sand and ideas presented by Ismael (1990). It is noted that the silt p-y curves were developed based on the theoretical basis alone without any validation from the full-scale test results. The soil resistance in different levels is calculated through equations 44 and 45.

$$p_u = \overline{A}\min(p_{sd}, p_{st}) + p_{uc} \tag{44}$$

$$p_m = B\min(p_{sd}, p_{st}) + p_{uc} \tag{45}$$

The parameters p_{sd} and p_{st} are calculated according to the cohesionless properties of the soil through the equations 24 and 25 as previously depicted in the Reese 1974 sand p-y model. The parameter p_{uc} is calculated according to the cohesive properties of the soil as the smallest value of equation 18 and 19 as depicted in the Welch and Reese 1972 stiff clay model. The coefficients A and B are defined according to figure 5. The initial linear portion of the displacement reaction curve is calculated according to equations 46 and 47.

$$p = k_{py} \cdot z \cdot y \tag{46}$$

$$k_{py} = k_c + k_\phi \tag{47}$$

Parameter k_{py} is subgrade modulus of the silt soil, k_c is the subgrade modulus contribution of the silt soil due to its cohesive properties while k_φ is the subgrade modulus contribution of the silt soil due to its cohesionless properties (Calculation of the subgrade modulus contribution factors is accomplished through figure 11). The parabolic portion following the initial linear behavior can be calculated through the use of equations 29-33. The displacement reaction curves of the p-y model derived by Reese and Van Impe for the scenario of sites consisting of silt soils is illustrated in figure 10.

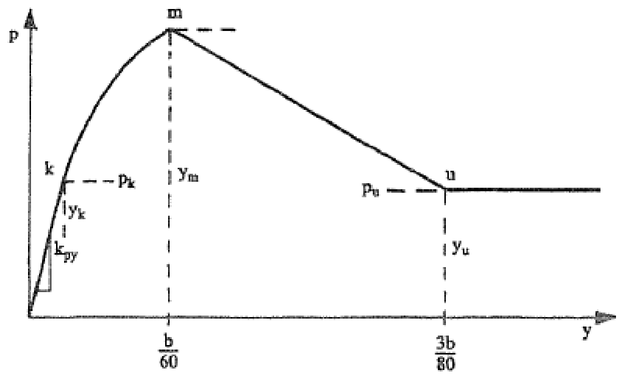

Figure 2.10: silt soil P-Y model as proposed by Reese and Van Impe (2000)

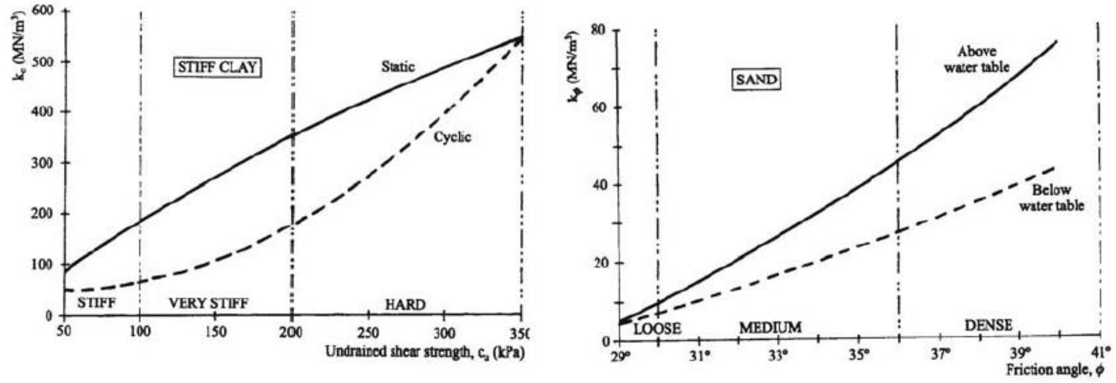

Figure 2.11: Subgrade modulus in a) cohesive soils b) cohesionless soils

2.2 multilayer soil profile

As the aforementioned P-Y models are capable of representing the nonlinear behavior of the soil explicitly for the homogeneous soil domain, additional steps are necessary for the expansion of the method in a multilayer site. A complete approach for such an expansion has been proposed by Georgiadis in 1986. According to the proposed method the soil ultimate resistance for each layer is calibrated accordingly in order to take into consideration the properties of the layers located above.

According to the proposed method the P-Y springs of the top layer are calculated according to the previously presented homogeneous P-Y models. However for the following soil layer the homogenous P-Y spring formulas are adjusted according to the layer properties located above them through the consideration of an equivalent depth in the mathematical formula of each P-Y spring (The effective stress is taken into account according to the actual depth of each layer and not according to the adjusted equivalent depth). The calculation of the adjusted initial depth of each layer is accomplished through the equations (48) and (49). As an initial step the force F_1 required to induce soil failure of a pile segment embedded to the bottom of the upper layer is calculated from equation 48.

$$F_1 = \int_0^{H_1} pu_1(h)\,dh \tag{48}$$

Where H_1 is the depth of the bottom of the 1st layer, pu_i(h) is the ultimate soil resistance according to the P-Y spring model of the first layer and h is the depth. As force F_1 has been calculated the adjusted depth h_2 of the same pile in a homogeneous soil with properties of the 2nd layer is calculated through equation 49 so that the force required to cause failure at a depth up to h_2 is equal to F_1.

$$\int_{o}^{h_2} Pu_2(h)\,dH = F_1 \tag{49}$$

The same procedure is iteratively applied at each intersection of two different layers until the function *F(z)* of force required to cause failure up to depth *z* is adjusted for the overall pile depth. The method is illustratively explained in Georgiadis publication through figure 11.

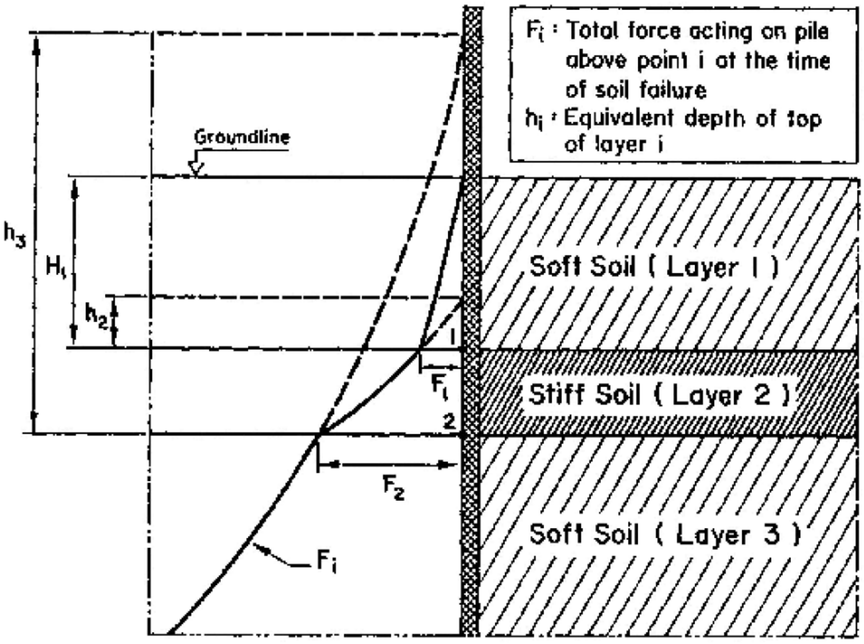

Figure 2.11: Georgiadis approach on the P-Y method implementation in multilayer soil profiles

2.3 battering of Piles

On the scenario of a single pile foundation with a battering angle a limited number of experimental publications have been accomplished in the past. The aforementioned publications in most scenarios directly provide adjustment factors on the soil resistance for each P-Y spring while others provide with a complete theoretical method appropriately calibrated according to experimental results. A detailed illustration of previously proposed adjustment factors based on experimental results is collectively presented in figure 12.

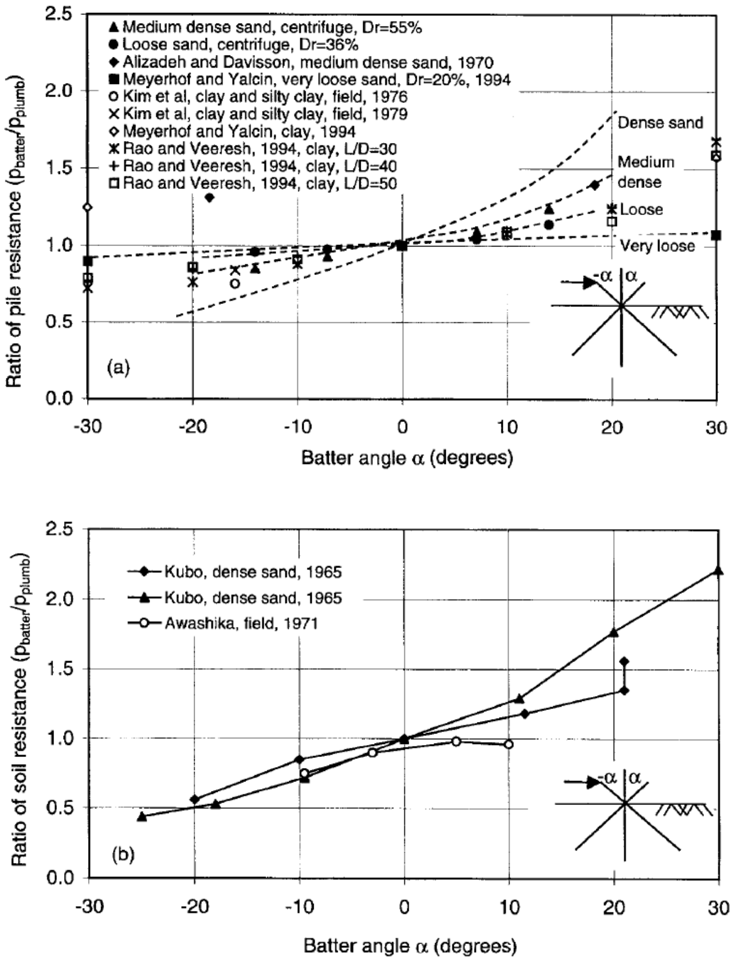

Figure 2.12: Factors proposed by different authors as multipliers on the ultimate soil resistance of the soil for different battering angles as depicted in Zhang et al (1999)

Due to the limitation of experimental results the selection of the appropriate literature adjustment factors can be accomplished individually for each P-Y model. On the current software implementation the proposed model developed by (Zhang et al 1999) was considered as the optimal scenario for the appropriate adjustment of the cohesionless P-Y models of Reese 1974 and API1993. According to the aforementioned approach the battering angle is affecting both the ultimate soil resistance along with the initial elastic stiffness of the P-Y plumb pile spring through the use of the same adjusting factor ψ. The adjusting factor can be calculated from the equation 50.

$$\psi = \lambda \frac{K_{pb}}{K_p} \tag{50}$$

Where Kpb and Kp are the passive pressure coefficients for the battering pile and plumb pile respectively, according to Coulomb's theory. Coefficient λ is an adjusting coefficient that accounts for the size of the sand's passive soil wedge through its relative density. The coefficient λ can be calculated from equation 51.

$$\lambda = 1 - f(Dr)\sin a \tag{50}$$

Where *a* is the battering angle of the pile and f(Dr) is a function of relative density of the cohesionless soil illustrated in figure 13a. Through the calculation of the coefficient ψ it is possible to calculate the adjusted P-Y model curve as depicted in figure 13b.

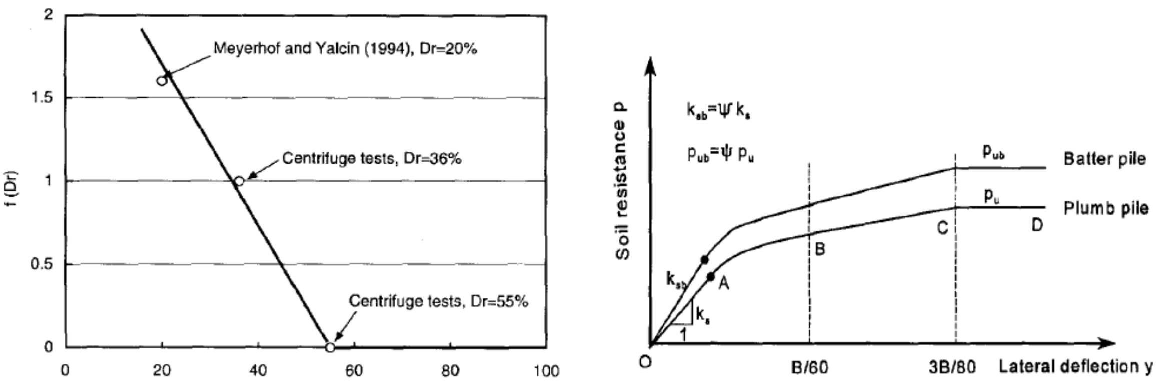

Figure 2.13: Factors proposed by different authors as multipliers on the ultimate soil resistance of the soil for different battering angles as depicted in Zhang et al (1999)

On the scenario of the clay models proposed by Matlock and Reese the Rao and Veeresh experimental results of piles driven in clay deposits are implemented as the adjustment factors due to the battering of the pile. On the specific case of the weak rock model proposed by Reese since soil specific experiments are not yet available the more general relation generated from Awoshika report of field tests is considered the safer approach.

3. Verification of software with Experimental results

3.1 Cox et al (1974)

The Cox et al (1974) experimental investigations on single piles under lateral excitation are included in the verification process of the cohesionless P-Y models implemented in the HelixPile software. In regard to the experimental configuration, the test site consisted of sandy clay seams underlain by a layer of firm gray clay and a layer of silty fine sand. Before the lateral load test, 2.44 m of clay layer were removed and backfilled with 0.76 m of sand. The sand at the test site varied from clean fine to silty fine, both exhibiting high relative density. The angle of internal friction, ϕ, was determined to be 39° degree, and the value of the submerged unit weight, γ′, was 1.06 tn/m³. The water table and ground levels were the same after the placement of the backfill. The test pile was hollow circular steel pile with a diameter of 0.61 m and a thickness of 9.5 mm.

In regard to the simulation of the experimental configuration in the HelixPile software, the Reese proposal was selected as the most efficient P-Y model for the specific soil properties. The subgrade modulus was derived by the HelixPile through the empirical correlation of K_{sub} with the angle of internal friction of the cohesionless soil as proposed in (Reese 1974). The comparison of the pushover results for the experimental data and the P-Y simulation are illustrated in figure 1b.

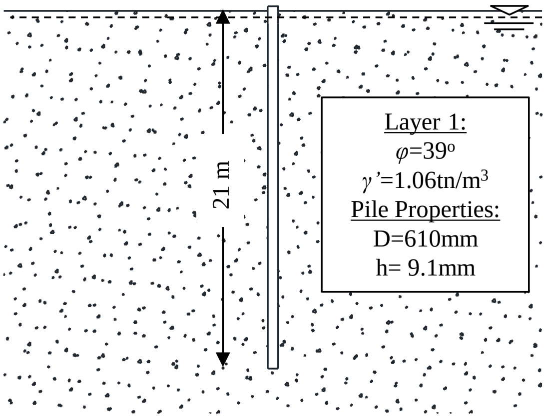

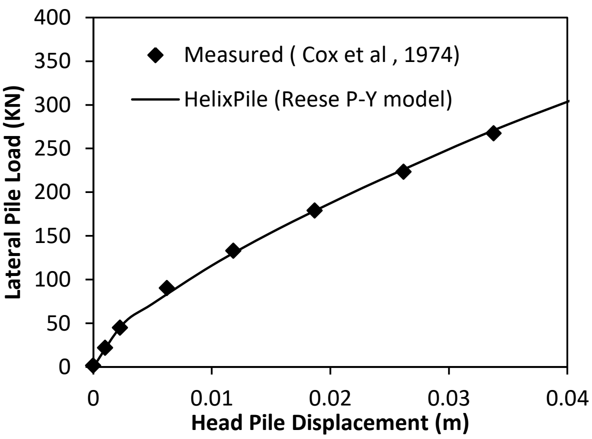

Figure 3.1:a) site and experiment configuration C1 b) comparison of measured results with P-Y simulation in the HelixPile Software

3.2 Price and Wardle (1981)

The Price and Wardle (1981) experimental investigations on single piles under lateral excitation are included in the verification process of the cohesive clay P-Y models implemented in the HelixPile software. The experiment measured the response of a steel pipe pile with diameter equal to 0.406m embedded in an overall length of 16.5m. The soil properties of the cohesive soil of the site were defined through in site measurement tests. According to the results of the tests the following undrained shear strength values of 44.1, 85.2, 80.6 and 133.3 KPa have been reported for the depths 0, 4.6, 6.2 and 19 m respectively.

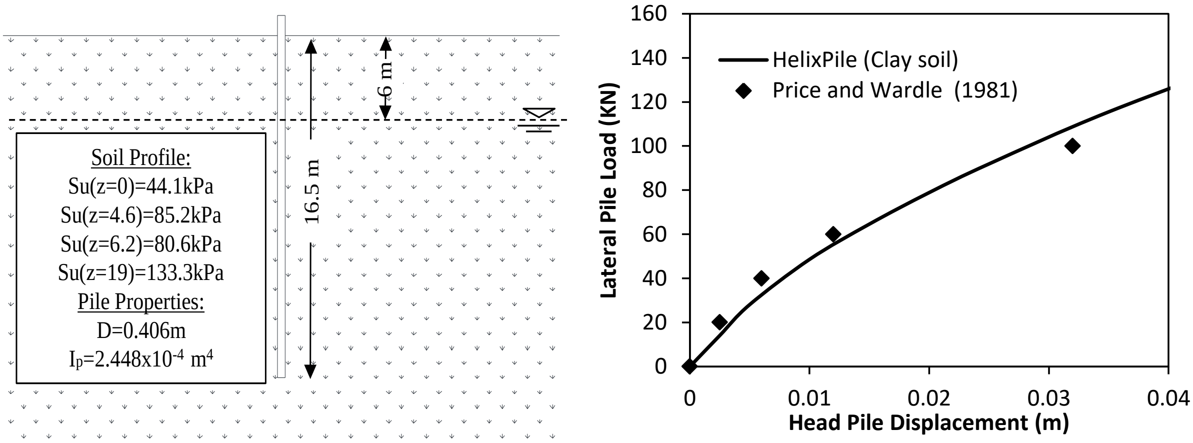

Figure 3.2:a) site and experiment configuration C2 b) comparison of measured results with P-Y simulation in the HelixPile Software

In regard to the simulation of the experimental configuration in the HelixPile software, four intermediate layers with constant properties were defined in order to appropriately simulate the increase of the undrained shear strength relative to the depth of the site. The calculation of the strain parameter which occurs at one half the maximum stress on laboratory undrained compression tests ε_{50} is accomplished through the empirical correlation to the undrained shear strength function for overconsolidated Clay deposits as proposed by (Reese and Van Impe 2001) . The appropriate stiff or soft clay P-Y models are selected for each individual layer according to the layers properties. The comparison of the pushover results for the experimental data and the P-Y simulation are illustrated in figure 2b.

3.3 Davisson and Gill (1963)

The multilayer capabilities of the HelixPile software are verified through the two layer site test performed in Austin, Texas (Davisson and Gill 1963). The experimental test consisted of the cyclic lateral loading of a 152mm diameter and 3.2mm thickness pipe section pile with embedded length equal to 4.9 meters. The soil profile is comprised by an initial stiff clay layer of 380mm thickness overlying medium dense sand. According to measurements on site the clay layer undrained shear strength was found to be equal to 96 KN/m^2 while the medium dense sand layer is defined by an angle of friction equal to 35° and subgrade modulus equal to 15.5MN/m^3.

Regarding the simulation of the experimental configuration in the HelixPile software, the Reese P-Y model was selected for the simulation of the cohesionless layer while the cohesive clay layer was simulated through the stiff clay model with no free water model. The comparison of the pushover results for the experimental data and the P-Y simulation are illustrated in figure 3b.

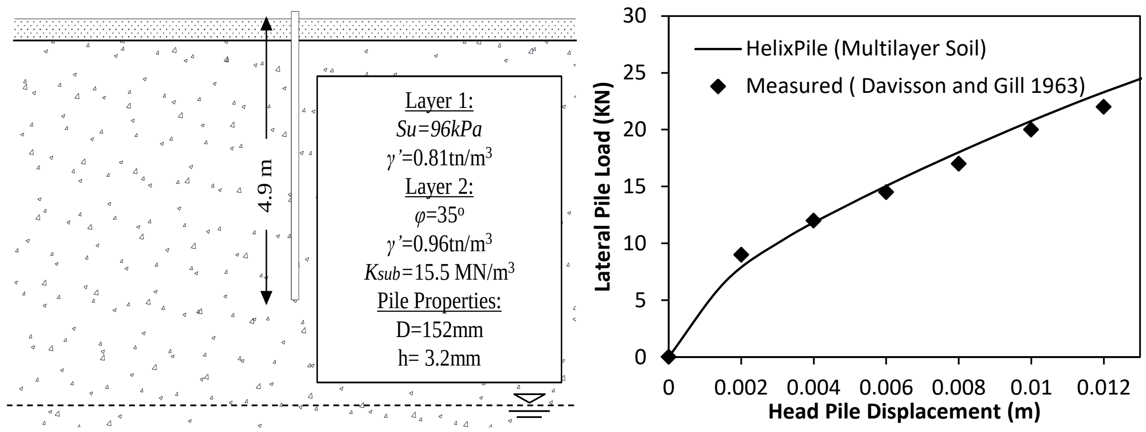

Figure 3.3:a) site and experiment configuration C3 b) comparison of measured results with P-Y simulation in the HelixPile Software

3.4 Mohammed Sakr (2010)

The (Sakr 2010) single pile experiments under lateral excitation are implemented in the verification process of the HelixPile software in order to estimate the accuracy of the numerical P-Y helical pile configuration. The comparison of the experimental and numerically simulated behavior of the single helical pile is calculated for two different piles and site locations included in the Sakr research paper. The ST23 experimental configuration consists of a 0.406m diameter steel pipe pile with double helixes of diameter equal to 0.813m, located in a four layer soil site as illustrated in figure 4a. The ST18 experimental configuration consists of the same diameter but different thickness steel pipe pile with one helix of diameter equal to 0.914m, located in a four layer site with different soil properties and layer thickness as illustrated in figure 5a.

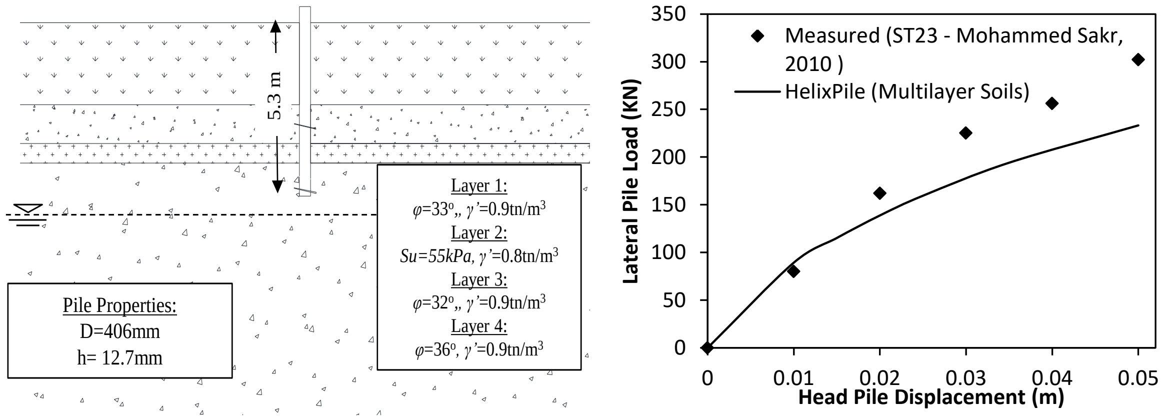

Figure 3.4:a) site and experiment configuration C4 – ST23 b) comparison of measured results with P-Y simulation in the HelixPile Software

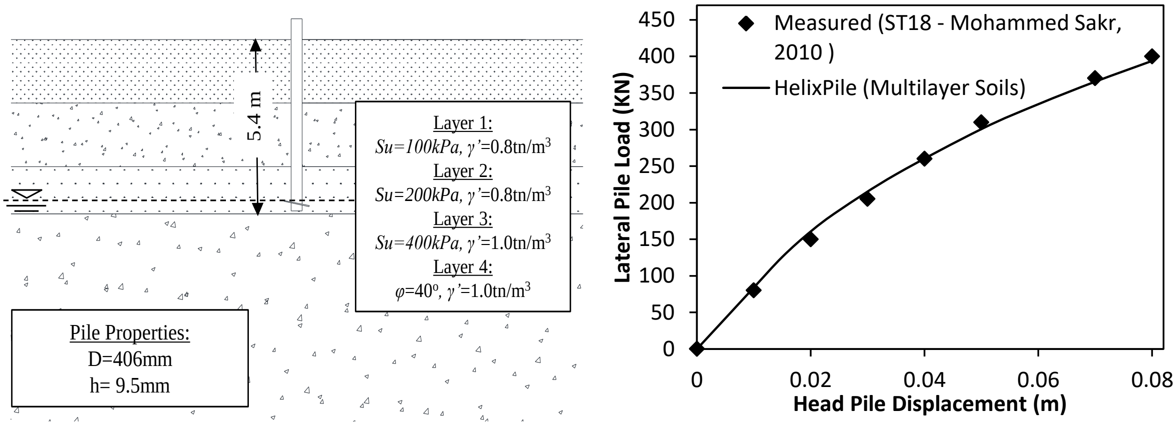

Figure 3.5:a) site and experiment configuration C4-ST18 b) comparison of measured results with P-Y simulation in the HelixPile Software

In regard to the simulation of the experimental configuration in the HelixPile software, the Reese P-Y model was selected as the modeling representation of the cohesionless soil layers while Matlock and Reese models where used for the cohesive soil layers simulation, where the stiff or soft clay model selection was accomplished in accordance to the undrained shear strength of each cohesive soil layer. The subgrade modulus essential to the cohesionless soils was derived by the HelixPile according to an empirical correlation with the angle of internal friction as proposed by (Reese 1974). The comparison of the pushover results for the experimental data and the P-Y simulation are illustrated in figure 4b and 5b.

3.5 Japan, the Committee on Piles Subjected to Earthquake (1965)

The Committee on Piles Subjected to Earthquake (1965) reported the results from testing a steel-pipe pile with a closed end that was jacked into the soil. The soil properties at the site in question along with the location of the water table are illustrated in figure 3.6.

Soil	γt	c'	Su	Φ'	Ksub	e50	Qu	RQD	krm
Name	(kN/m3)	(kPa)	(kPa)	(deg)	(kN/m3)	-	(kPa)	(%)	-
Clay 1 (UND.)	14.9	-	29.93	0	-	0.02	-	-	-
Clay 2 (UND.)	14.9	-	35.2	0	-	0.02	-	-	-
Clay 3 (UND.)	14.9	-	40.47	0	-	0.02	-	-	-

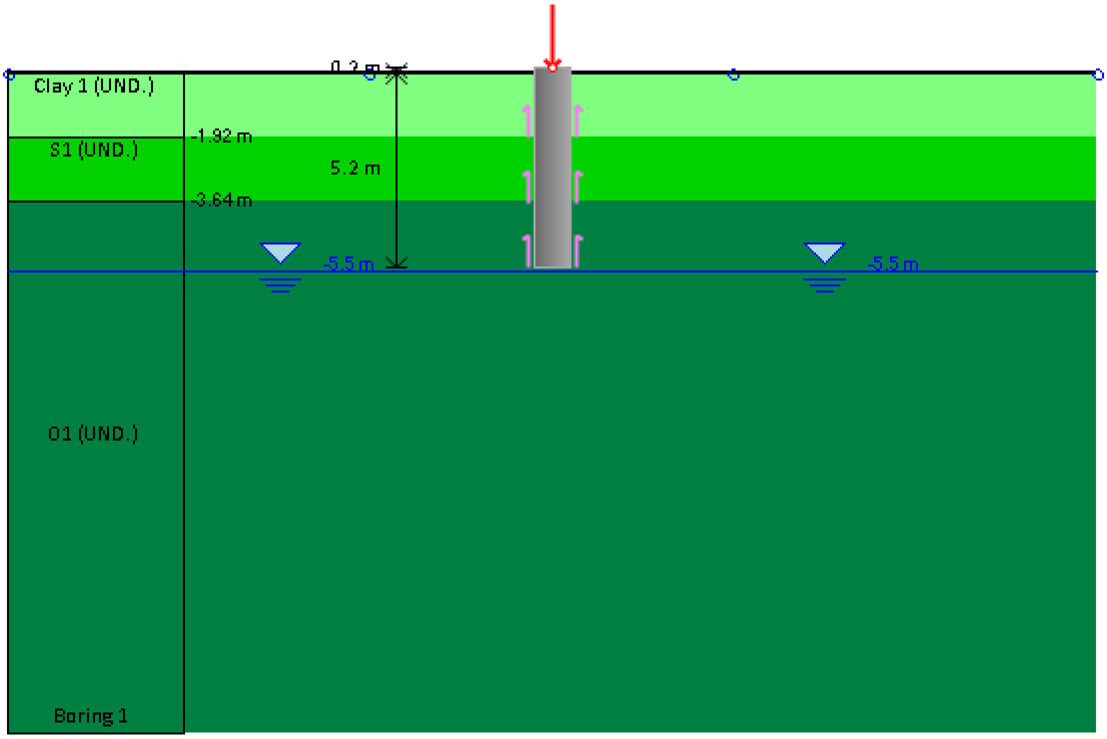

Figure 3.6 : Assembly of pile foundation, Case study "1" Japan (1965)

The pile has an overall length of 5.5m while the lateral loading was applied at a distance of 0.201m above ground line. The properties of the pipe section are illustrated in figure 3.7. The steel pipe section had a modulus of elasticity equal to E=200 GPa and a yielding stress equal to Fy=235Mpa.

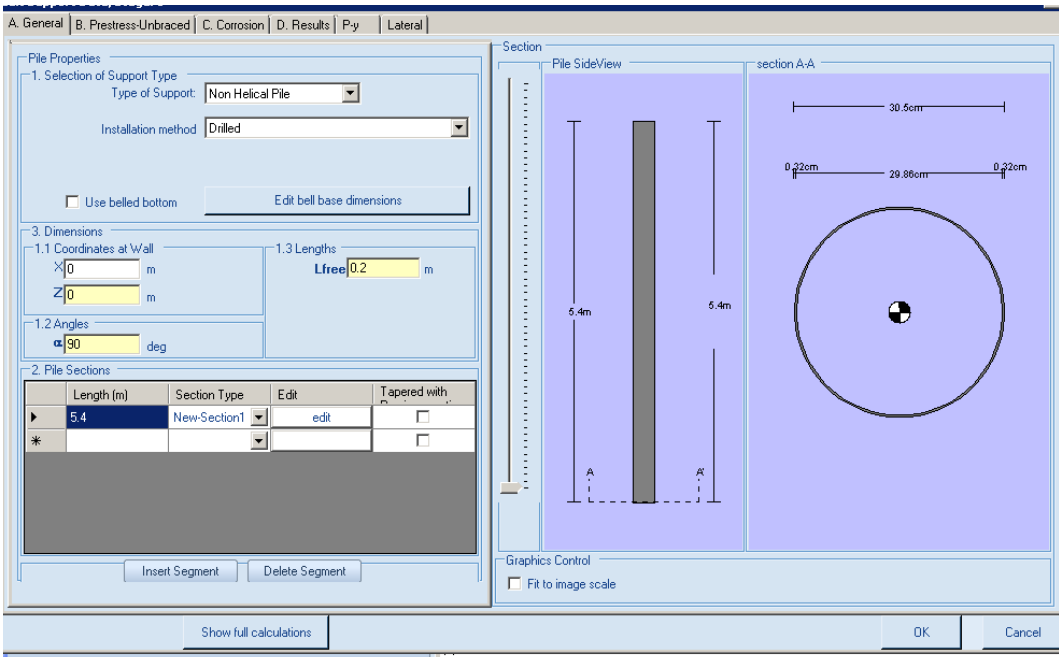

Figure 3.7: Properties of pile Case study "1" Japan (1965)

The P-Y results of the force applied at the head of the pile to the pile head lateral deflection for both the experimental results and the results obtained from the DeepFND analysis are illustrated in figure 3.8.

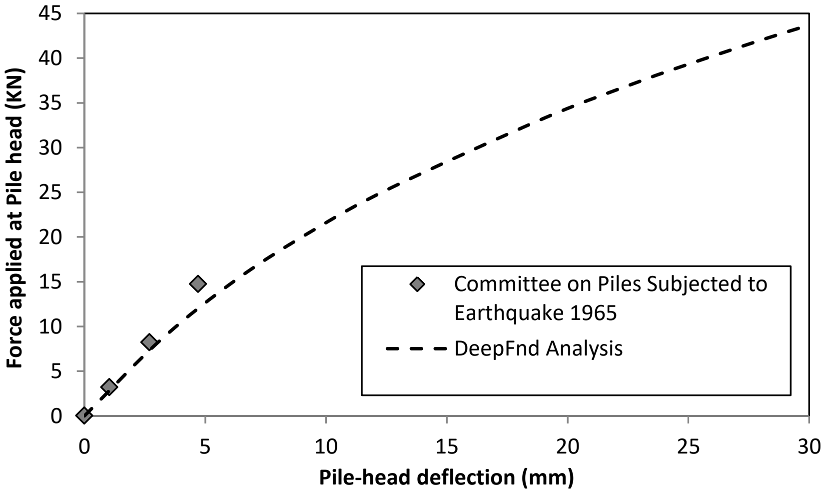

Figure 3.8: Comparison of experimental and computational results ,Force to deflection relationship , Case study "1" Japan (1965)

The P-Y results of the force applied at the head of the pile to the pile head lateral deflection for both the experimental results and the results obtained from the DeepFND analysis are illustrated in figure 3.9.

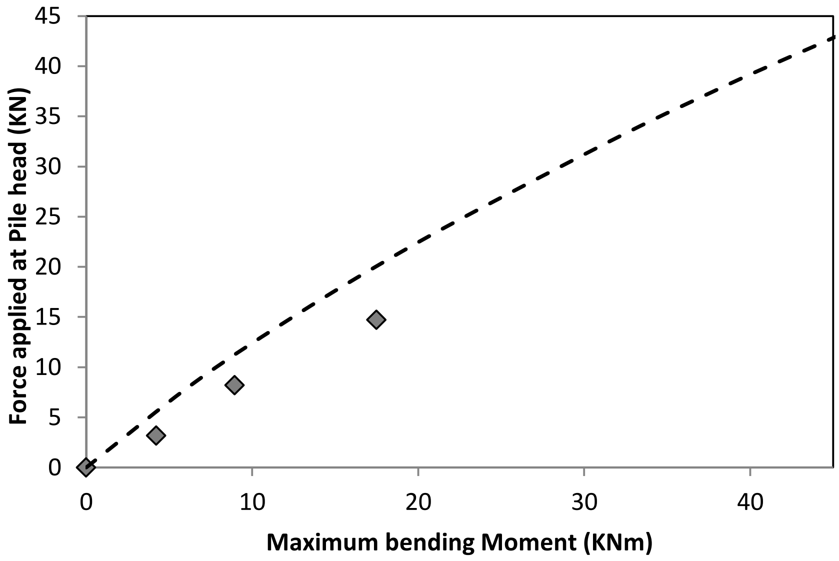

Figure 3.9: Comparison of experimental and computational results, Force to maximum bending moment relationship, Case study "1" Japan (1965)

3.5 Matlock(1970)

Matlock (1970) lateral-load tests include a steel-pipe pile experimental configuration driven in clays near Lake Austin Texas. The soil properties at the site in question along with the location of the water table are illustrated in figure 3.10.

Soil Name	γt (kN/m3)	c' (kPa)	Su (kPa)	Φ' (deg)	Ksub (kN/m3)	e50 -	Qu (kPa)	RQD (%)	krm -
Soil 1 (UND.)	20	-	39	0	-	0.012	-	-	-

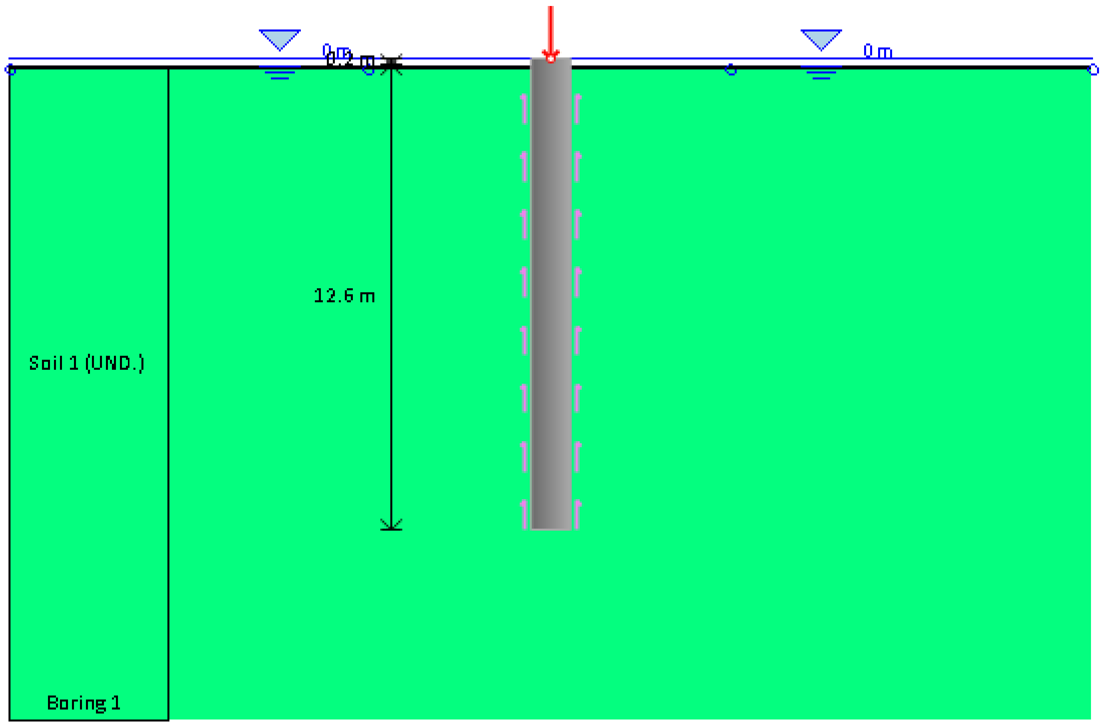

Figure 3.10: Assembly of pile foundation, Case study "3" Lake Austin (1970)

The pile has an overall length of 12.6m while the lateral loading was applied at a distance of 0.0635m above ground line. The properties of the pipe section are illustrated in figure 3.11. The steel pipe section had a modulus of elasticity equal to E=200 GPa and a yielding stress equal to Fy=235Mpa.

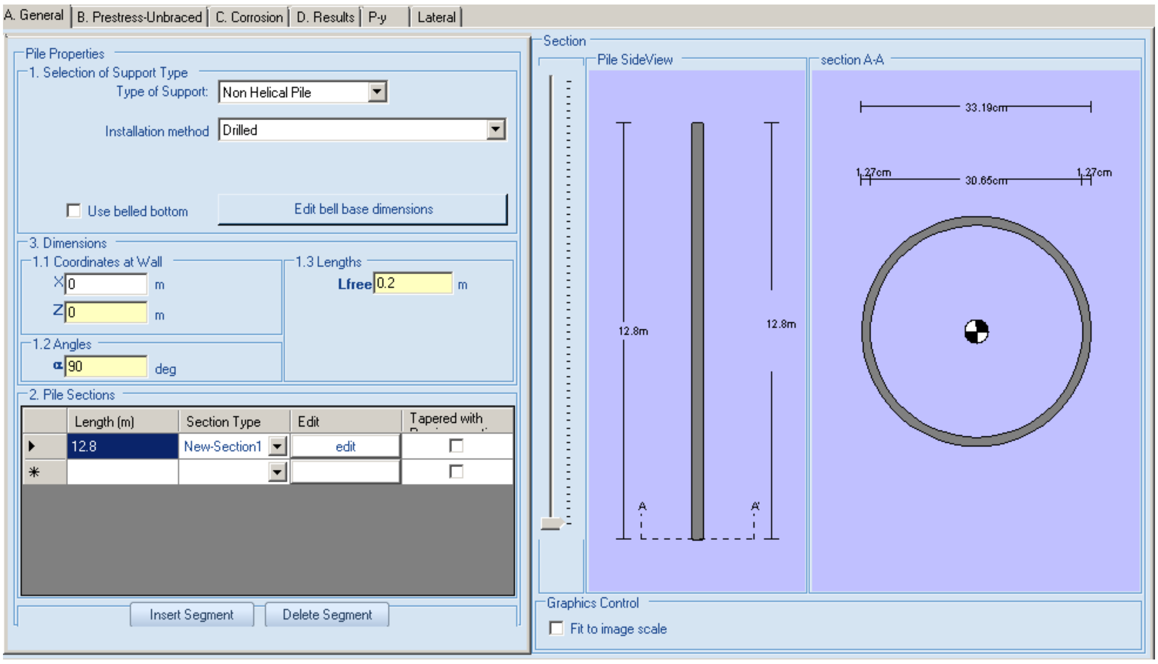

Figure 3.11 : Properties of pile Case study “3” Lake Austin (1970)

The P-Y results of the force applied at the head of the pile to the pile head lateral deflection for both the experimental results and the results obtained from the DeepFND analysis are illustrated in figure 11.

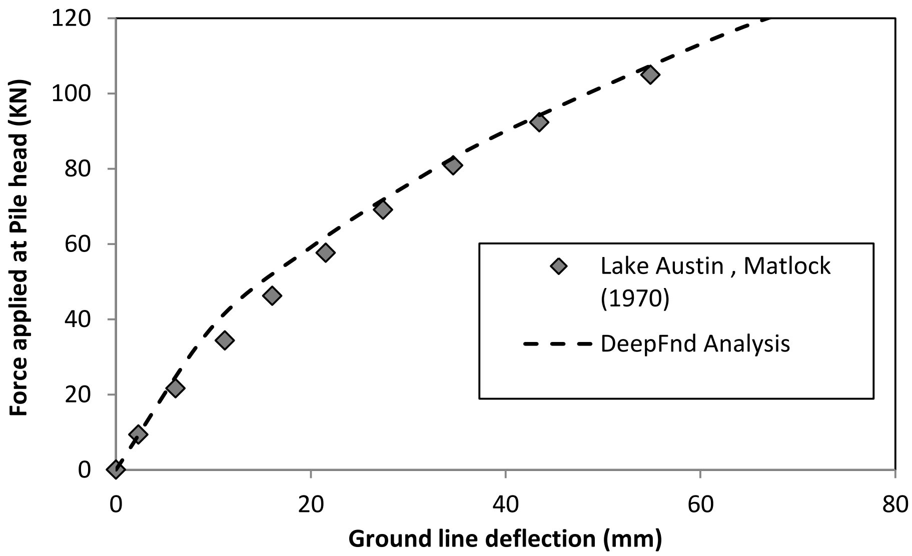

Figure 3.12 : Comparison of experimental and computational results ,Force to deflection relationship , Case study “3” Lake Austin (1970)

The P-Y results of the force applied at the head of the pile to the pile head lateral deflection for both the experimental results and the results obtained from the DeepFND analysis are illustrated in figure 16.

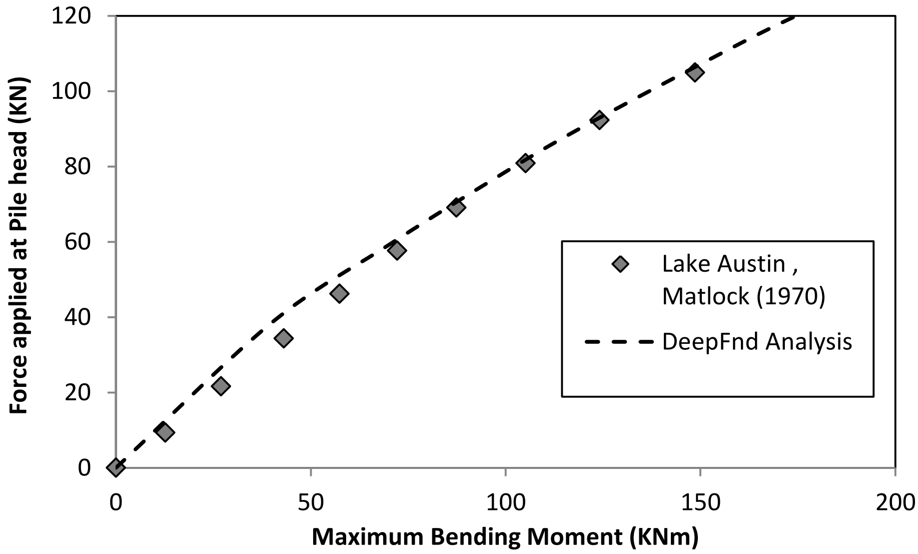

Figure 3.13 : Comparison of experimental and computational results, Force to maximum bending moment relationship, Case study "3" Lake Austin (1970)

3.6 Alcacer do Sol, Portugal et al (1993)

The pile tested at Lake Austin was removed and installed at Sabine in a site of soft clay properties [4]. The soil properties at the site in question along with the location of the water table are illustrated in figure 3.14.

Soil	γt	c'	Su	Φ'	Ksub	e50	Qu	RQD	krm
Name	(kN/m3)	(kPa)	(kPa)	(deg)	(kN/m3)	-	(kPa)	(%)	-
CLAY 1 (UND.)	16	-	20	0	-	0.02	-	-	-
SAND 1	19	20	-	30	9000	-	-	-	-
CLAY 2 (UND.)	16	-	32	0	-	0.02	-	-	-
Sand 2	20	5	-	35	15000	-	-	-	-

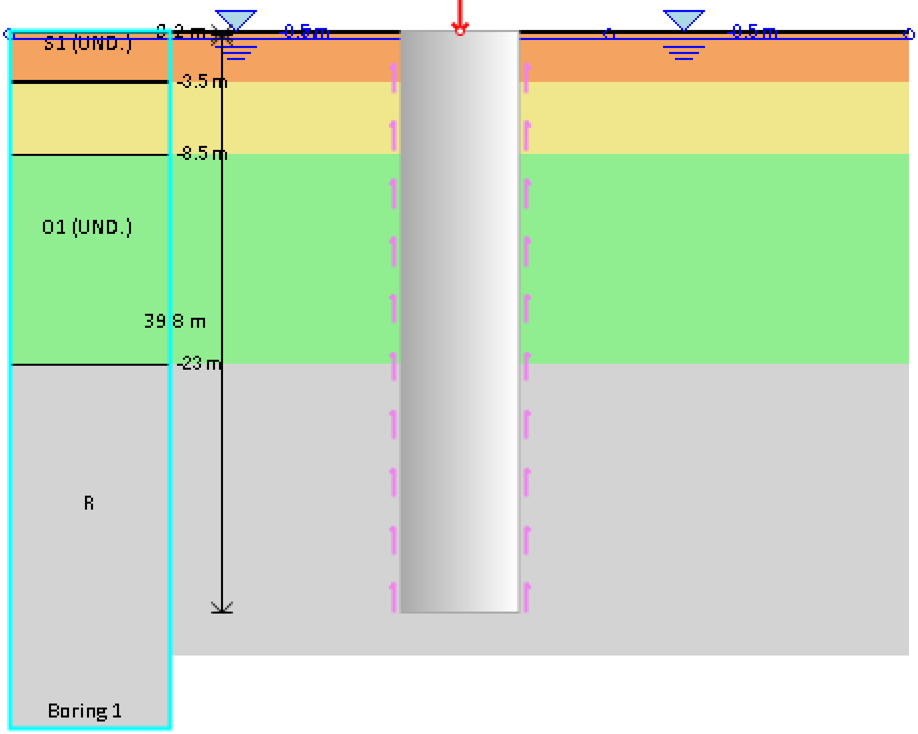

Figure 3.14 : Assembly of pile foundation, Case study "5" Alcacer do Sol (1979)

The pile has an overall length of 40m while the lateral loading was applied at a distance of 0.2m above ground line. The properties of the pipe section are illustrated in figure 18. The pile had a diameter of 1.2 m. It was reinforced with 35bars with a diameter of 25 mm. The strengths of the concrete and steel were reported to be 33.5 MPa and 400 MPa, respectively. The cover of the rebars was taken as 50 mm.

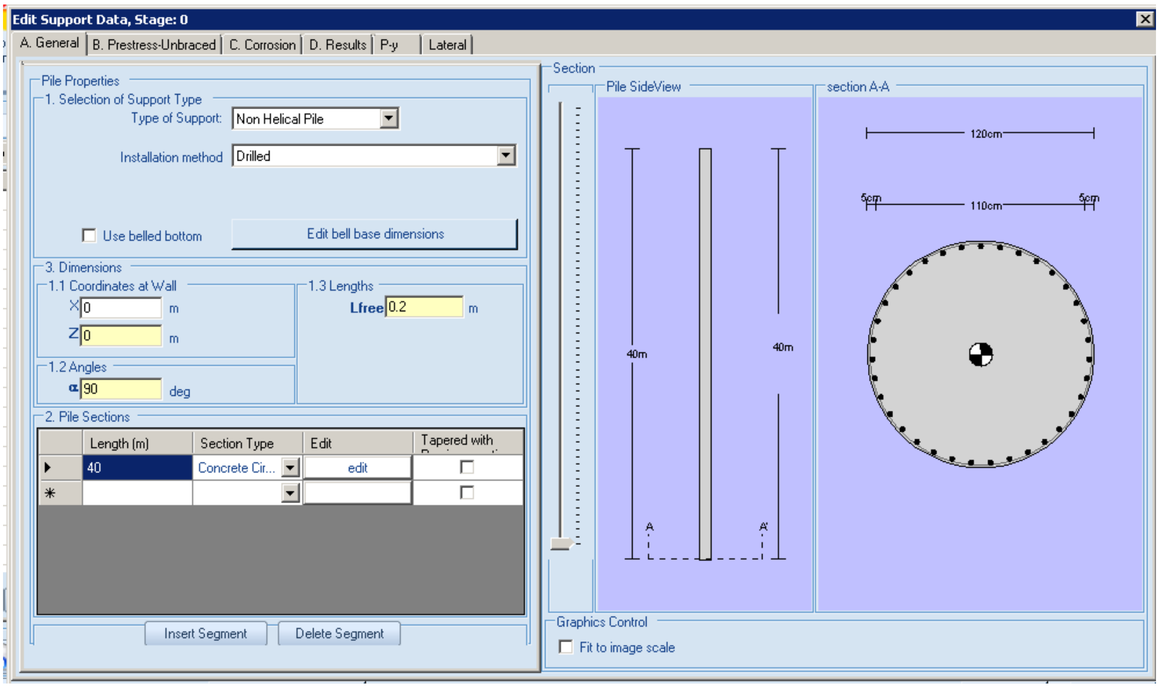

Figure 3.15 : Properties of pile Case study "5" Alcacer do Sol (1979)

The P-Y results of the force applied at the head of the pile to the pile head lateral deflection for both the experimental results and the results obtained from the DeepFND analysis are illustrated in figure 20.

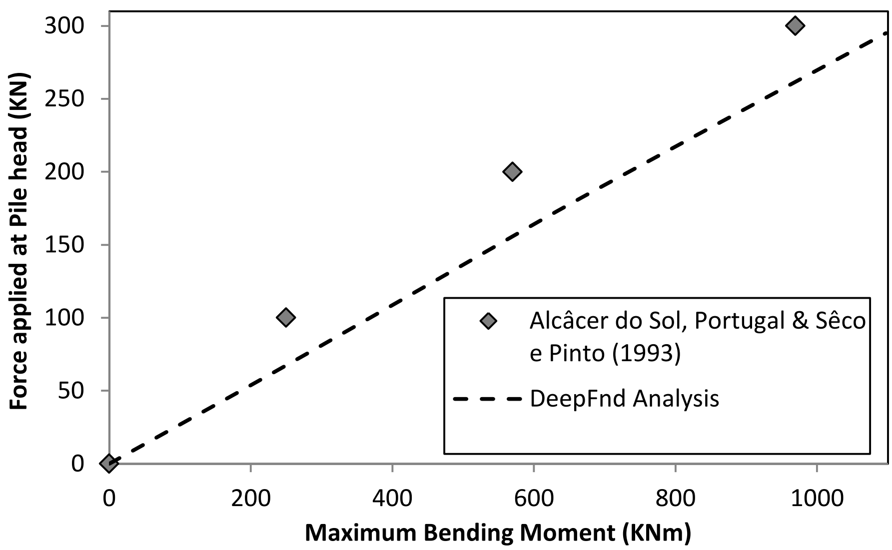

Figure 3.16 : Comparison of experimental and computational results, Force to maximum bending moment relationship, Case study "5" Alcacer do Sol (1979)

4. References

Davisson, M. T., and Gill, H. L. (1963). “Laterally loaded piles in a layered soil.” *J. Soil Mech. and Found. Div.*, ASCE, 89(3), 63-94.

Georgiadis, M. (1983). “Development of p-y curves for layered soils.” *Proc. of the Conference on Geotechnical Practice in Offshore Engineering*, ASCE , 536-545

Matlock, H. (1970). “Correlations for design of laterally loaded piles in soft clay.” *Proc., 2nd Annu. Offshore Technology Conf., Paper No. OTC 1204*, Houston, Texas, 577-594.

O’Neill, M. W., and Murchison, J. M. (1983). “An evaluation of p-y relationships in sands.” A report to the American Petroleum Institute.” *PRAC 82-41-1*, University of Houston, Texas.

Reese, L. C., Cox, W. R., and Koop, F. D. (1974). “Analysis of laterally loaded piles in sand,” *Proc. 6th Offshore Technology Conference, Paper 2080*, Houston, Texas, 473-483.

Reese, L. C., Cox, W. R. and Koop, F. D. (1975). “Field testing and analysis of laterally loaded piles in stiff clay.” *Proc., 7th Offshore Technology Conf., Paper No. OTC 2321*, Houston, Texas, 671-690.

Reese, L. C., and Van Impe, W. F. (2001). *Single Piles and Pile Group under Lateral Loading*. A. A. Balkema, Rotterdam, 463 p.

Reese, L. C., and Welch, R. C. (1975). “Lateral loading of deep foundation in stiff clay.” *J. Geotech. Engrg. Div.*, ASCE, 101(7), 633-649.

Welch, R. C., and Reese, L. C. (1972). “Laterally loaded behavior of drilled shafts.” *Research Report 3-5-65-89*, Center for Highway Research, University of Texas, Austin.

Committee on Piles Subjected to Earthquake 1965. Lateral Bearing Capacity and Dynamic Behavior of Pile Foundation. Architectural Institute of Japan (in Japanese): 1-69.

Cox, W.R., L.C. Reese & B.R. Grubbs 1974. Field testing of laterally loaded piles in sand. *Proceedings of the Offshore Technology Conference, Houston, Texas*, paper 2079

Meyer, B.J. 1979. Analysis of single piles under lateral loading. Thesis, University of Texas,Austin.

Analysis and design of piles under lateral loads. *Proceedings of the II International Geotechnical Seminar on Deep Foundations on Bored and Auger Piles (BAP II), Ghent, Belgium:* 309-313.

Mohammed Sakr 2010, *Lateral Resistance of High Capacity Helical Piles* – Case Study, GEO2010

.